

the same equation predicts arresting crater growth when it had advanced to only about 68% of its size in a vacuum (with the added assumption that the length scale, L , over which the forces act begin after the crater has grown to 50% of its final size). It is important to recognize that equation (1) predicts that atmospheric deceleration on the curtain increases with increasing crater size because $L \sim R_v$ and $t_e \sim R_v^{1/2}$; consequently, $\ln(v/v_0) \sim R_v^{1/2}$.

Tests: Several observations are consistent with the inferences drawn from the laboratory experiments and the simple analogy. First, nonballistic ejecta emplacement near the rim reflects deceleration and collapse of the ejecta curtain. Craters 70 km in diameter on Venus exhibit this transition within 0.25 crater radii of the rim. Second, as atmospheric effects become extreme, the combined roles of rim/wall collapse and decreased ejecta run-out should result in increasing collapse of the uplifted rim and inner ejecta facies with increasing size. Third, diameter-to-depth relations for complex craters on Venus should parallel simple craters on other planets (Fig. 1).

References: [1] Gault D. E. et al. (1968) In *Shock and Metamorphism of Natural Materials* (B. M. French et al., eds.), 87–100, Mono, Baltimore. [2] Schultz P. H. and Gault D. E. (1990) In *GSA Spec. Pap. 247* (V. Sharpton and P. Ward, eds.), 239–261. [3] McGetchin T. R. et al. (1973) *EPSL*, 20, 226–236. [4] Oberbeck V. R. et al. (1975) *Moon*, 12, 19–54. [5] Schultz P. H. (1992) *JGR*, 97, 975–1006. [6] Schultz P. H. (1990) *LPSC XXI*, 1097–1098. [7] Schultz P. H. (1992) *JGR*, in press. [8] Orphal D. et al. (1980) *Proc. LPSC 11th*, 2302–2323.

N93-14371 1484373

EFFECT OF IMPACT ANGLE ON CENTRAL-PEAK/PEAK-RING FORMATION AND CRATER COLLAPSE ON VENUS.
Peter H. Schultz, Brown University, Department of Geological Sciences, Providence, RI 02912, USA.

Although asymmetry in ejecta patterns and crater shape-in-plan are commonly cited as diagnostic features of impact angle [1,2], the early-time transfer of energy from impactor to target also creates distinctive asymmetries in crater profile with the greatest depth uprange [1]. In order to simulate gravity-controlled crater growth, laboratory experiments use loose particulate targets as analogs for low-strength material properties following passage of the shock. As a result, impact crater diameter D in laboratory experiments generally is many times greater than the impactor diameter $2r$ (factor of 40), and early-time asymmetries in energy transfer from oblique impacts are consumed by subsequent symmetrical crater growth, except at the lowest angles ($<2.5^\circ$). Such asymmetry is evident for oblique ($<60^\circ$ from horizontal) impacts into aluminum where $D/2r$ is only 2 to 4. Because cratering efficiency decreases with increasing crater size [3,4] and decreasing impact angle [1], large-scale planetary craters (40–80 km) should have transient excavation diameters only 6–10 times larger than the impactor [5]. At basin scales, $D/2r$ is predicted to be only 3–5, i.e., approaching values for impacts into aluminum in laboratory experiments. As a result, evidence for early-time asymmetry in impactor energy transfer should become evident on planetary surfaces, yet craters generally retain a circular outline for all but the lowest impact angles.

Evidence for energy-transfer effects in fact occurs on the Moon and Mercury but depends on scale. For simple craters (Messier, Toricelli), crater depth is greatest uprange with a steep uprange and shallow downrange wall slope. For complex craters (Buys-Ballot, Tycho, King), the central peak is offset uprange (corresponding to the greatest depth) but the wall exhibits greater failure uprange

(corresponding to higher slope). Moreover, the central peak in King Crater is breached downrange. For two-ringed basins (Bach on Mercury), the interior ring is breached downrange with evidence for greater rim/wall failure uprange, observations also consistent with the oblong Crisium Basin on the Moon [6]. The cratering record on Venus allows extending such observations where $D/2r$ should be further reduced because of the greater gravity and perhaps effects of the atmosphere [7].

Craters on Venus: Figure 1 illustrates a 42 km-diameter crater with central peak offset uprange, a steep (narrow) uprange inner wall slope, and a broad but gently sloping downrange wall. Since the radar look direction is nearly transverse to impact direction, the observed asymmetry reflects the impact process and not imaging perspective. Figure 2a illustrates a similar uprange offset of a central peak ring and a similar contrast in the uprange/downrange wall. Figure 2b, however, reveals a reversal in this pattern for a larger crater: a downrange offset of the inner ring. It is proposed that this reversal reflects more extensive rim/wall failure as crater depth and uprange slope exceeds a critical value. This proposal is consistent with the concentric scarps within the crater, transform faults crossing the peak ring, and step faulting beyond the rim. The examples in Figs. 1 and 2 are typical for Venus. Exceptions occur only where topography also plays a role or where the impactor was clearly multiple.

If the central massifs (peaks and peak rings) reflect the region of maximum depth, then the size of this disruption may reflect the size of the impactor [7,8]. As a test, crater diameter referenced to peak-ring diameter should increase with decreasing impact angle (judged from the missing sector uprange and the overall degree of ejecta asymmetry) as cratering efficiency decreases. If peak-ring diameter reflects a response to impactor kinetic energy or potential energy (depth), then this ratio should decrease with decreasing impact angle. As shown in Fig. 3, peaking diameter comprises a greater fraction of crater diameter as impact angle decreases; consequently, it is suggested that peak rings indeed may provide markers of impactor size. This marker most likely reflects a limiting (but common) value of peak stress created during penetration [8].



Fig. 1. Crater (42 km in diameter) with central peak offset uprange and exhibiting contrast between steep, narrow and shallow, broad downrange wall. Arrows indicate crater rim. C1-15 S009. Radar look direction from the left; arrow indicates impact direction.

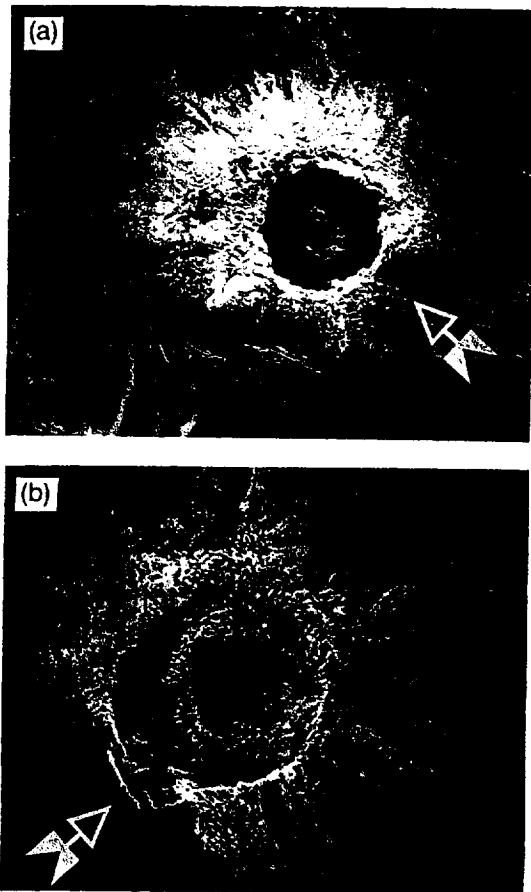


Fig. 2. (a) Crater (50 km diameter) exhibiting a partial central peak ring offset uprange (from lower right) C1-60N 263. Radar look direction is from upper left. (b) Larger crater (103 km diameter) exhibiting central peak ring offset downrange from present rim, opposite to occurrence in (a) and Fig. 1. Reversal in position is related to enhanced rim/wall collapse uprange that widens and circularizes the crater around the deepest portion of the transient crater cavity, which occurs uprange. Further crater widening follows pre-existing structural grain. C1-30N 135.

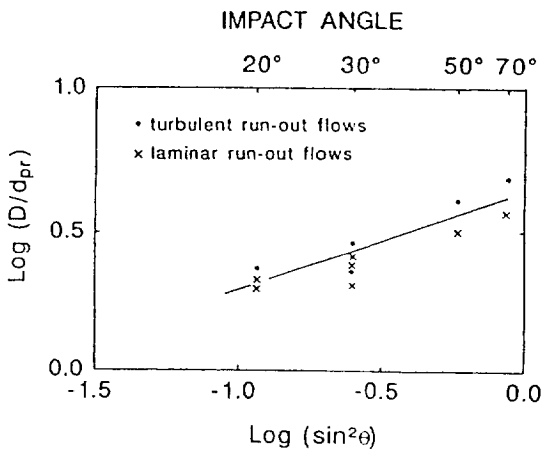


Fig. 3. Effect of impact angle (from horizontal) on the transverse diameter of the central peak ring d_{cp} referenced to crater diameter. As impact angle decreases (based on degree of ejecta symmetry), size of central peak ring becomes larger relative to crater diameter. Such a trend is expected if central peak ring reflects the size of impactor and cratering efficiency decreases impact angle.

The enhanced uprange rim/wall collapse illustrated in Fig. 2b (and numerous other large oblique impacts on Venus) provides insight for why most craters exhibit a circular outline even though early-time energy transfer comprises a larger fraction of crater growth. Failure of the uprange rim/wall in response to the oversteepened wall and greater floor depth circularizes crater outlines. The rectilinear and conjugate scarp on the pattern uprange rim, however, indicates failure along preimpact stresses. Hence, a corollary is that peak shock levels and particle motion may be reduced uprange during oblique impacts due to the downrange motion of the impactor, analogous to time dilation.

References: [1] Gault D. E. and Wedekind J. A. (1978) *Proc. LPSC 9th*, 3843–3875. [2] Moore H. J. (1979) *U.S. Geol. Surv. Prof. Pap.* 812–13, 47 pp. [3] Gault D. E. and Wedekind J. A. (1977) In *Impact and Explosion Cratering* (D. Roddy et al., eds.), 1231–1244, Pergamon, New York. [4] Holsapple K. A. and Schmidt R. M. (1987) *JGR*, 92, 6350–6376. [5] Schultz P. H. and Gault D. E. (1991) *Meteoritics*, 26. [6] Wichman R. W. and Schultz P. H. (1992) *LPSC XXIII*, 1521–1522. [7] Schultz P. H. (1988) In *Mercury* (F. Vilas et al., eds.), 274–335, Univ. of Arizona, Tucson. [8] Schultz P. H. (1992) *JGR*, in press.

N93-14372 08 374

IMPACT-GENERATED WINDS ON VENUS: CAUSES AND EFFECTS. Peter H. Schultz, Brown University, Department of Geological Sciences, Box 1846, Providence RI 02912, USA.

The pressure of the dense atmosphere of Venus significantly changes the appearance of ejecta deposits relative to craters on the Moon and Mercury. Conversely, specific styles and sequences of ejecta emplacement can be inferred to represent different intensities of atmospheric response winds acting over different timescales. Three characteristic timescales can be inferred from the geologic record: surface scouring and impactor-controlled (angle and direction) initiation of the long fluidized run-out flows; nonballistic emplacement of inner, radar-bright ejecta facies and radar-dark outer facies; and very late reworking of surface materials. These three timescales roughly correspond to processes observed in laboratory experiments that can be scaled to conditions on Venus (with appropriate assumptions): coupling between the atmosphere and earlytime vapor/melt (target and impactor) that produces an intense shock that subsequently evolves into blast/response winds; less energetic dynamic response of the atmosphere to the outward-moving ballistic ejecta curtain that generates nonthermal turbulent eddies; and late recovery of the atmosphere to impact-generated thermal and pressure gradients expressed as low-energy but long-lived winds. These different timescales and processes can be viewed as the atmosphere equivalent of shock melting, material motion, and far-field seismic response in the target.

Early Processes (Direct Effects of Blast and Fireball): Under vacuum conditions, the fate of the impactor is generally lost; even on the Earth, most impact melt sheets exhibit little trace of the impactor. The dense atmosphere of Venus, however, prevents escape of the impactor through rapid deceleration of ricochet debris and containment of the vapor cloud [1,2]. Figure 1a illustrates the time required for the atmospheric blast front to decelerate to the speed of sound as a function of crater size, where k is the fraction the initial impactor energy (KE_i) coupled to the atmosphere (E_A). On Venus, the shock front dissipates before the crater finishes forming. If the blast is created by deceleration and containment of early high-speed ejecta (downrange jetting and ricochet/vapor), then it will precede ejecta emplacement and should exhibit a source area offset